JOURNAL OF CATALYSIS 64, 173–183 (1980)

Catalytic Properties of Molybdenum-Containing Zeolites in Epoxidation Reactions

I. Catalysts Preparation and Characterization

PEI-SHING EUGENE DAI AND JACK H. LUNSFORD

Department of Chemistry, Texas A & M University, College Station, Texas 77843

Received September 27, 1979; revised February 11, 1980

Molybdenum ions have been introduced into a Y-type zeolite by using a solid–solid exchange method, in which the ultrastable zeolite or normal hydrogen zeolite was mixed with $MoOCl_4$ and heated to 400°C. The physicochemical properties of the resulting $MoHY_u$, MoHY, and MoCoHY zeolites were investigated by infrared, EPR and photoelectron spectrscopy and by X-ray diffraction techniques. Comparison of the XPS signals of Mo in an impregnated sample with those of an ion-exchanged sample confirms that the molybdenum ions were indeed exchanged into zeolites. The binding energies of the Mo_{3d} doublet at 232.7 and 235.8 eV show that the Mo ion was mainly present as Mo(VI); however, EPR spectra of the fresh, dehydrated molybdenum-exchanged zeolites reveal that about 3.5% of the molybdenum was present as the Mo(V) ion. After being used as a catalyst for the epoxidation of cyclohexene, all of the low-valent Mo ions were oxidized to Mo(VI), whereas there was no change in the oxidation state of Co(II) ions. A band at 900 cm^{-1} in the infrared spectra of MoHY and MoCoHY zeolites is attributed to the Mo═O bond vibration. Based on the spectroscopic data, two structures of molybdenum ions in Mo-exchanged zeolites are postulated. Structural analysis of the zeolites by X-ray diffraction and infrared spectrscopy indicates that the solid-phase exchange reaction resulted in some loss in crystallinity for all of the Mo-exchanged zeolites.

INTRODUCTION

Molybdenum-containing catalysts are used in many industrial processes (*1, 2*). For example, molybdenum complexes such as naphthenates are active catalysts for the epoxidation of olefins with organic hydroperoxides. Thus, the increasing interest in zeolites as catalysts for oxidation reactions and the commercial interest in selective epoxidation of olefins stimulated us to explore a method for exchanging molybdenum into zeolites. Because on is able to obtain a uniform distribution of metal ions in a zeolite by ion exchange, and since unsaturated coordination for transition metal ions is zeolites is possible, this support appears to be ideal for the preparation of a heterogeneous molybdenum catalyst.

Transition metal ions of high oxidation state are generally difficult to exchange into zeolites since few cationic forms are available as simple metal salts, and those exist only in strongly acidic solutions where exchangeable cations must compete effectively with protons and where many zeolites are unstable. For example, a tetravalent thorium-exchanged Y zeolite, prepared by ion-exchanging NaY with thorium nitrate solution, showed some loss of crystallinity (*3*).

Molybdenum-containing zeolites have been prepared by impregnation (*4*). Furthermore, several methods including conventional aqueous ion exchange, vapor-phase dispersion, and incorporation of molybdenum into the lattice have been used in an attempt to form zeolites containing well-dispersed Mo, but these have not produced a crystalline material with high surface area (*5*). It has been shown, however, that molybdenum ions can be introduced into zeolites by adsorption of molybdenum hexacrabonyl in a hydrogen Y

0021-9517/80/070173-11$02.00/0

zeolite (HY) with subsequent thermal decomposition (*6, 7*).

Clearfield and co-workers (*8, 9*) have demonstrated that solid–solid reactions between the hydrogen form of an ion-exchange material and transition metal chlorides afford an alternative way for incorporating transition metal ions into the ion-exchanger. The driving force for this reaction is the formation of gaseous HCl. They also reported that the crystal structure of a copper-exchanged NaY zeolite, prepared by this technique, remained essentially intact.

In those cases where zeolites tend to lose crystallinity, ultrastable Y zeolites (HY_u) are known to have higher hydrothermal stability and acid resistance. Recently, the preparation and physical properties of a lanthanum, hydrogen-exchanged ultrastable Y zeolite ($LaHY_u$) has been reported (*9–11*). The resulting zeolite exhibited high surface area and crystallinity.

In the present study, the solid–solid exchange reaction of molybdenum chlorides with both HY_u and HY zeolites has been carried out. These molybdenum-exchanged Y zeolites and molybdenum, cobalt-exchanged zeolites have been employed as catalysts for selective epoxidation of cyclohexene with molecular oxygen (*12*). The electron paramagnetic resonance (EPR) technique was used to identify paramagnetic molybdenum ions and paramagnetic oxygen species upon adsorption of molecular oxygen on the dehydrated molybdenum-exchanged zeolites. X-Ray powder diffraction and infrared spectroscopy were employed in a structural analysis of the zeolites. A study utilizing X-ray photoelectron spectroscopy (XPS) was undertaken to determine the location of molybdenum ions, as well as the oxidation states of metal ions in zeolites.

EXPERIMENTAL

The ammonium-exchanged Y zeolites were prepared by treating an NH_4NaY zeolite (Linde Y-6Z, Lot No. 373856) with 1 *M* $(NH_4)_2SO_4$ solution two times at 75°C for 24 hr. After the second exchange the NH_4Y samples were washed with deionized water to remove excess electrolyte and dried at room temperature. The ammonium Y zeolites were treated with aqueous $Co(NO_3)_2$ solutions of different concentrations at 75°C for 24 hr. After filtration the resulting cobalt, ammonium-exchanged Y zeolites ($CoNH_4Y$) were rinsed and dried at room temperature. Both the NH_4Y and $CoNH_4Y$ zeolites were deaminated at 350°C for 12 hr in a muffle furnace to produce hydrogen Y (HY) zeolites and cobalt-hydrogen Y (CoHY) zeolites. The ultrastable Y zeolite was prepared by following procedure A of McDaniel and Maher (*13*) in which structural aluminum is hydrothermally placed in exchange sites.

The hydrogen forms, HY, HY_u, and CoHY, were intimately ground together with anhydrous molybdenum pentachloride ($MoCl_5$) in the air. The resulting mixture was then dehydrated at 150°C for 2 hr and heated at 400°C for 10 hr in flowing helium. The exit gases were passed through a standardized NaOH solution to collect the HCl that was evolved. Anhydrous molybdenum pentachloride, purchased from ICN Pharmaceutical, was used without further purification.

The degree of exchange of cobalt and molybdenum was determined by digesting the zeolites in a mixture of 10 *M* HF and 2 *M* citric acid solutions. The metal content of these solutions was analyzed using atomic absorption spectrophotometry. The samples are designated, for example, as $Mo_{1.6}Co_{3.5}HY$, where the subscripts indicate the number of cobalt ions and molybdenum ions per unit cell.

The supported molybdenum chloride catalysts were prepared by impregnating the inorganic solid (γ-alumina, silica–alumina, and NaY zeolite) with the desired amount of $MoCl_5$ dissolved in tetrahydrofuran (THF) under ambient conditions. The solvent THF was removed under vacuum. An NaY zeolite impregnated with 2.6% by

weight of $MoCl_5$ corresponds to 15% of the cation exchange capacity of the zeolite.

The experimental method used for the epoxidation of cyclohexene in the liquid phase is described in the succeeding paper (*12*). The fresh and used zeolite materials mentioned in this paper refer to the zeolites before and after they were employed as catalysts for the catalytic reaction.

In the EPR experiments, zeolite samples were dehydrated by heating to 400°C in increments of 100°C/hr under a vacuum of 10^{-5} Torr. EPR spectra were recorded at −196°C using a Varian E-6S spectrometer. The g values are reported relative to a phosphorus-doped silicon standard with $g = 1.9987$. Spin concentrations were obtained by double integration of the recorded EPR spectrum and comparison with the known spin concentration of the standard.

The crystallinity of the zeolite powders was checked by means of X-ray powder diffraction data obtained on a Norelco powder diffractometer with Cu$K\alpha$ radiation at 35 kV and 14 mA. For the measurement of the framework vibration, the zeolites were mixed with KBr in the proportion zeolite:KBr = 1:100 and pressed into a wafer under a pressure of 1×10^3 kg/cm^2. The infrared spectra were recorded using a Beckman IR-9 spectrophotometer in the transmission mode. The accuracy of the band positions was estimated to be ±5 cm^{-1}.

For the XPS experiments, the pretreatment of zeolite wafers was performed in a quartz cell. Fresh zeolite catalysts were dehydrated by heating to 400°C in increments of 100°C/hr under a vacuum of 6×10^{-6} Torr. The used catalysts were degassed at 65°C overnight to less than 1×10^{-5} Torr. After the pretreatment the wafer was transferred under an N_2 atmosphere in a glove box to a Hewlett–Packard 5950 ESCA spectrometer. Monochromatic Al$K\alpha$ X rays (1486.6 eV) were employed in this spectrometer. The pressure in the analyzer chamber during any run was less than 4×10^{-9} Torr. Charge compensation was achieved by flooding the sample with nearly zero-kinetic-energy electrons. Typical collecting times were 3 hr for the Mo_{3d} line, 10 hr for the Co_{2p} line, 0.5 hr for the Si_{2p} line, and 1 hr for the Al_{2s} line.

Binding energies were referenced to a gold spot which was deposited on the sample. The $4f_{7/2}$ line of Au was assigned a binding energy of 84.0 eV. The Si_{2s} (154.0 eV) and C_{1s} (285.0 eV) lines from the zeolite were used as secondary standards. Binding energies were reproducible to ±0.2 eV for the Mo_{3d} line and ±0.3 eV for the Co_{2p} line.

For a sample of infinite thickness the relative intensity of the two characteristic peaks is given by Eq. (1) (*14*):

$$\frac{I_1}{I_2} = \frac{n_1}{n_2} \times \frac{\lambda_1}{\lambda_2} \times \frac{\sigma_1}{\sigma_2} \times \frac{S_1}{S_2}, \qquad (1)$$

where λ is the mean free path of the photoelectrons of kinetic energy E_c, S is the transmission factor of the spectrometer for an energy E_c, σ is the effective ionization cross section, and n is the atomic concentration of the element. In this study, the transmission factor of the spectrometer and the mean free path of electrons were assumed to be the same for elements Si, Al, and Mo. Therefore, the surface atomic ratio can be estimated from Eq. (2):

$$\frac{n_1}{n_2} = \frac{I_1}{I_2} \times \frac{\sigma_2}{\sigma_1}, \qquad (2)$$

where the peak intensity I was normalized to a 1-hr scan and the photoionization cross sections reported by Scofield were used (*15*).

RESULTS AND DISCUSSION

Stoichiometry for the reaction of molybdenum oxychloride with HY zeolites Molybdenum pentachloride is readily converted to oxychlorides, hydroxychlorides, or other oxygen-containing products upon exposure to low concentrations of air or water (*16*). During the grinding and mixing of $MoCl_5$ with the hydrogen-containing Y zeolites in the air, much of the $MoCl_5$ was transformed to $MoOCl_4$ as indicated by the

green color of the sample. Upon dehydration of the mixture of HY zeolite with $MoOCl_4$ at 150°C for 2 hr in the flowing helium, the pH value of the dilute aqueous NaOH solution remained constant. After raising the temperatures to 400°C for 2 to 3 hr, there was a large change in the pH value, which indicated that HCl gas was evolved during that period.

The total amount of HCl produced was equal to about 80% of the theoretical amount of chlorine based on the weight of $MoCl_5$. This result indicates that approximately 4 moles of HCl were liberated per mole of molybdenum chloride. It is consistent with the reaction of $MoOCl_4$ with the hydroxyl groups and the remaining zeolitic water, as written in Eqs. (3a) and (3b):

$$MoOCl_4 + 4HO{-}Si \rightarrow O{=}Mo(O{-}Si\leftarrow)_3 + 4HCl + O{-}Si\leftarrow \quad (3a)$$

$$MoOCl_4 + 4H_2O \rightarrow MoO(OH)_4 + 4HCl. \quad (3b)$$

The number of surface OH groups has been estimated to be 1.5×10^{19} per gram of zeolite for a 1-μm particle (*17*). The amount of $MoOCl_4$ added to the zeolite, corresponding for example to 8.5% of the exchange capacity, is twice as large as the total number of surface hydroxy groups. Therefore, the $MoOCl_4$ must also react with OH groups in the large cavities.

EPR studies. After degassing the freshly prepared $Mo_{1.6}HY_u$ at 400°C, an EPR spectrum of Mo(V) shown in Fig. 1a was observed. This spectrum is characterized by $g_\perp = 1.956$ and $g_\parallel = 1.884$. The amount of Mo(V) present in a dehydrated $Mo_{1.6}HY$ zeolite was estimated to be 3.5% of the total molybdenum content. Reduction of the dehydrated $Mo_{1.6}HY_u$ zeolite by 400 Torr of H_2 at 480°C resulted in a fourfold increase in the Mo(V) signal as shown in Fig. 1b.

Exposure of the dehydrated $Mo_{1.6}HY_u$ to 10 Torr of O_2 at 25°C gave the EPR signal of O_2^- with $g_1 = 2.0173$, $g_2 = 2.0092$, and $g_3 = 2.0034$ (Fig. 1c). The O_2^- ion is known to be coordinated to Mo(VI) (*18*). No EPR signal of the O^- ion was observed upon addition of 25 Torr N_2O to a reduced $Mo_{1.6}HY_u$ sample at 25°C and subsequent thermal treatment at 90°C (*19*). The intensity of the Mo(V) signal, however, decreased remarkably upon exposure to N_2O at 90°C, which indicates oxidation to Mo(VI).

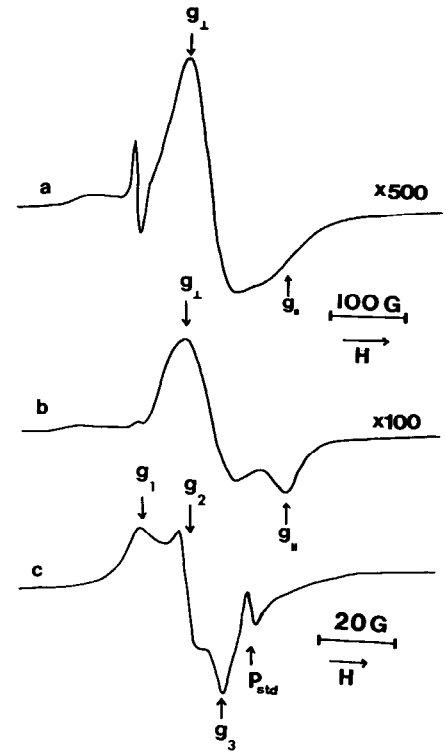

FIG. 1. EPR spectra: (a) after degassing the freshly prepared $Mo_{1.6}HY_u$ at 400°C; (b) sample reduced in 400 Torr of H_2 at 480°C; (c) after exposure of the dehydrated sample to 10 Torr of O_2 at 25°C.

The asymmetric EPR signal of Mo(V) shows that the Mo(V) ion is in an axially symmetric environment. The g values are consistent with molybdenum ions in either distorted octahedral or tetrahedral symmetry (*20*). The latter seems more likely, at least for part of the molybdenum, since only Mo(V) ions in a distorted tetrahedral environment are able to transfer electrons to O_2 (*21*). The effects of nitrous oxide and oxygen also provide information on the

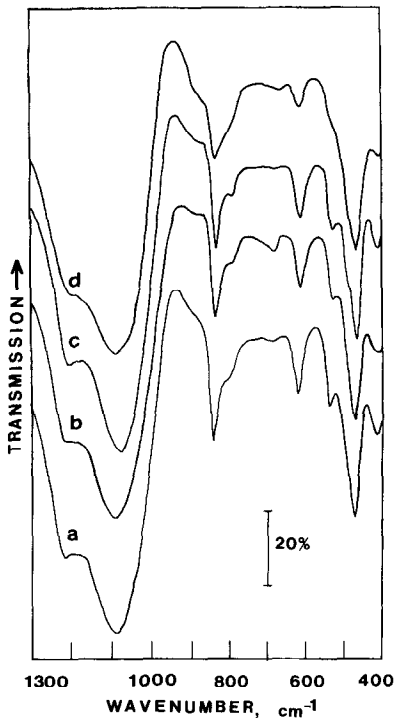

FIG. 2. Infrared spectra of (a) HY_u, (b) $Mo_{0.83}HY_u$, (c) $Mo_{1.6}HY_u$, and (d) $Mo_{3.1}HY_u$ zeolites.

location of the molybdenum ions since N_2O and O_2 can enter only the large cavities of the zeolite at moderate temperatures. It follows that the Mo(V) ions must be located on the external surface of the zeolite or within the large cavities.

Mid-infrared spectra of zeolites. The mid-infrared spectra of HY_u and several $MoHY_u$ zeolites are shown in Fig. 2. The framework infrared spectrum of HY_u shown in Fig. 2a is in agreement with the data of Scherzer and Bass (*22*). Absorption bands were observed at 410, 465, 530, 615, 835, 1070, and 1200 cm^{-1}. Vibrational and other motions of the zeolite framework have been extensively studied by Flanigen *et al.* (*23*). The midinfrared vibrations are classified into (i) internal vibrations of the TO_4 tetrahedra that tend to be structure insensitive and (ii) vibrations of external linkages between tetrahedra that are sensitive to variation in the framework structure. The vibrations are not specifically assigned to SiO_4 or AlO_4 groups, but rather to the vibrations of (Si, Al)O_4 groups designated as TO_4. According to Flanigen (*23*), the asymmetric and symmetric stretching vibrations of internal TO_4 units for NaY zeolite are in the regions of 950–1250 and 650–720 cm^{-1}, respecitvely. For external linkages they occur in the regions of 1050–1150 and 750–820 cm^{-1}. The bands near 420 to 500 cm^{-1} are assigned to the deformation modes of TO_4. The bands in the regions of 500–650 and 300–420 cm^{-1} are assigned to the double rings of tetrahedra forming the hexagonal prisms and the large pore openings, respectively.

With an increase in Mo exchange level, the bands at 530, 615, and 835 cm^{-1}, due to vibrations of the double rings and symmetric stretching of external linkages, exhibited a decrease in intensity as shown in Figs. 2b–d. The decrease in intensity of the structure-sensitive bands is attributed to a loss in crystallinity as a result of the solid–solid exchange reaction. In the spectrum of $Mo_{3.1}HY_u$, shown in Fig. 2d, the band at 530 cm^{-1} became a weak shoulder and the band at 835 cm^{-1} became broad. These two bands seem to be the most sensitive to the loss in crystallinity.

Pichat *et al.* (*24*) observed a linear increase in frequency of the stretching O–(Al, Si)–O vibrations (around 1050 and 800 cm^{-1}) with decreasing Al content of aluminum-deficient zeolites. This quantitative relationship can yield the number of framework Al atoms for ultrastable zeolites. From the band positions at 835 and 1070 cm^{-1} observed for the HY_u and $MoHY_u$ zeolites, one may conclude that the Al content of these samples was less than 26 Al ions per unit cell.

The framework infrared spectra of $NaNH_4Y$, NH_4Y, HY, and $Mo_{1.2}HY$ zeolites are depicted in Fig. 3. The spectrum of the NH_4Y zeolite showed the appearance of structure-sensitive bands at 580, 790, and 1150 cm^{-1} (Fig. 3b). The intensity of the 580-cm^{-1} band decreased when NH_4Y zeolite was deaminated to form HY and exposed to

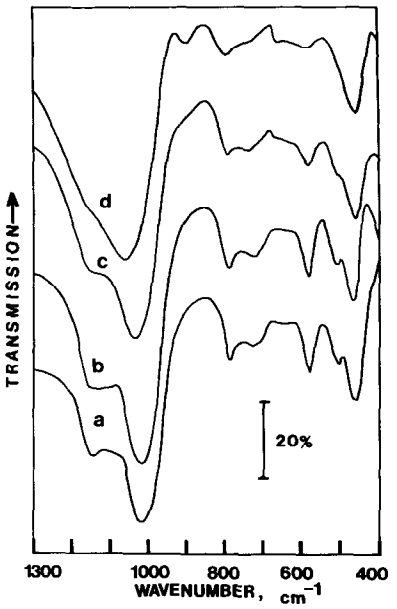

FIG. 3. Infrared spectra of (a) NH_4NaY, (b) NH_4Y, (c) HY, and (d) $Mo_{1.2}HY$ zeolites.

air (Fig. 3c). a similar change was also observed for the 790-cm^{-1} band. After exchanging the molybdenum into the HY zeolite, the relative intensity of the 580-cm^{-1} band decreased significantly, and the shoulder at 1150 cm^{-1} became very weak. It is important, however, to note that a new band appeared near 900 cm^{-1} as shown in Fig. 3d.

The infrared spectra of a series of MoCoHY zeolites with different Mo loading were similar to that of the $Mo_{1.2}HY$ in Fig. 3d; however, the structure-sensitive bands at 580, 790, and 1150 cm^{-1} in all of the MoCoHY zeolites were more pronounced than those in $Mo_{1.2}HY$ zeolite. With an increase in Mo loading there was no appreciable change in the relative intensities of the structure-sensitive bands. The new band at 900 cm^{-1}, which appeared as a weak shoulder in the spectrum of MoCoHY zeolite, increased in amplitude with Mo loading.

Gallezot *et al.* (*7*) interpreted an absorption band at 895 cm^{-1} as evidence for the formation of an Mo^{n+}–O_2^- bond; however, Primet (*25*) attributed a shift of the T–O vibrational band from 1035 toward 900 cm^{-1} in an RhNaY zeolite to the local deformation of a T–O bond caused by an oxygen–cation interaction. Mitchell and Trifiro (*26*) demonstrated that the frequency of an Mo=O bond vibration depends upon the coordination number and the number of terminal oxygen atoms on the molybdenum. The tetrahedral *cis*-dioxo molybdenum(VI) complexes have Mo=O frequencies in the ranges 876–913 and 909–943 cm^{-1} (*27*). Since the intensity of the 900-cm^{-1} band increased with increasing Mo loading, it must be associated with the molybdenum ions within the zeolites. By analogy with more conventional inorganic compounds we assign the absorption band at 900 cm^{-1} to an Mo=O bond vibration.

Flanigen *et al.* (*28*) have shown a correlation between the X-ray crystallinity and the integrated intensities of the structure-sensitive or external-linkage vibrations for NaY zeolite during thermal decomposition. In comparison with their spectra, one can estimate that the crystallinity in the $MoHY_u$

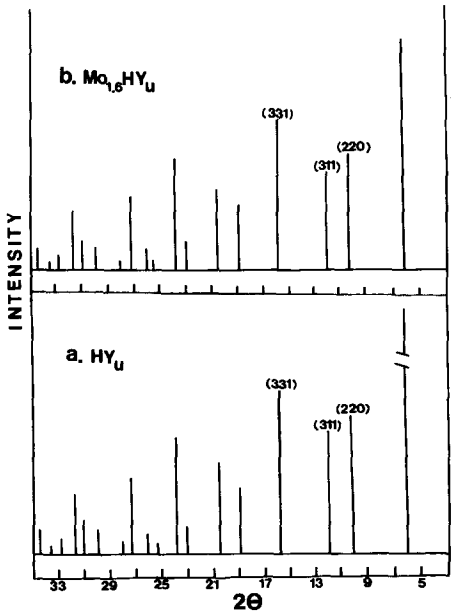

FIG. 4. X-Ray powder diffraction patterns for HY_u and $Mo_{1.6}HY_u$ zeolites.

samples was reduced at most by 20% whereas the crystallinity was reduced by more than 40% in the MoHY and MoCoHY zeolites.

X-Ray diffraction data. Typical X-ray powder diffraction patterns for HY_u and $Mo_{1.6}HY_u$ zeolites are shown in Fig. 4. The peaks with Miller indexes (331), (440), (533), (642), and (555) have *d*-spacings of 5.7, 4.4, 3.8, 3.3, and 2.8 Å. The unit cell constant decreased gradually from 24.67 Å for $NaNH_4Y$ to 24.56 Å for HY and then 24.34 Å for the HY_u zeolite.

Table 1 presents the relative intensities of selected peaks for all of the zeolites that were studied, using the starting material $NaNH_4Y$ as the reference. Since the line intensities are reported for the identical instrumental conditions of the X-ray diffractometer and the full width at half-maximum of every peak remained constant for all of the zeolites, the change in crystallinity is evident from this table for a number of samples, both before and after exchange with $MoOCl_4$. With increasing Mo loading, a decreasing crystallinity of MoCoHY zeolites was observed. The loss of crystallinity was less in the $MoHY_u$ samples than in the corresponding MoHY with the same Mo loading, which is consistent with the higher acid stability of the ultrastable Y zeolite. In the series of HY, MoHY, and MoCoHY zeolites, a substantial loss in crystallinity may result from dehydroxylation and rehydration of HY in the air, as well as from the high acidity produced in the exchange reaction with $MoOCl_4$.

TABLE 1

Crystallinity Changes in Various Mo-Containing Zeolites

Samples	*d*-spacing				
	5.67 Å	4.38 Å	3.78 Å	3.31 Å	2.85 Å
	$I/I(NaNH_4Y) \times 100$[a]				
$NaNH_4Y$	100	100	100	100	100
NH_4Y	100	96.7	100	93.8	89.8
HY	62.3	46.7	51.0	37.0	47.5
$Co_{6.6}HY$	65.8	55.0	58.7	58.4	52.5
$Mo_{0.75}Co_{3.6}HY$	41.2	35.6	38.0	38.5	33.9
$Mo_{1.6}Co_{3.5}HY$[b]	30.6	28.3	29.3	29.2	25.4
$Mo_{1.6}Co_{3.5}HY$[c]	29.4	28.3	30.4	26.1	25.4
$Mo_{2.9}Co_{3.5}HY$	27.1	25.0	26.0	26.1	20.3
$Mo_{3.7}Co_{3.5}HY$	22.3	18.3	21.7	21.5	16.9
$Mo_{1.2}HY$	17.6	13.3	16.3	13.8	13.5
HY_u	78.8	61.6	52.2	46.1	39.0
$Mo_{0.83}HY_u$	68.2	56.7	47.8	41.5	37.3
$Mo_{1.6}HY_u$[d]	89.4	70	65.2	57.0	54.2
$Mo_{1.6}HY_u$[e]	71.8	53.3	50	46.1	40.7
$Mo_{3.1}HY_u$	31.8	25	25	18.5	20.3

[a] *I* is the peak height in arbitrary units.
[b] Fresh catalyst, before the cyclohexene oxidation.
[c] Used catalyst, after the cyclohexene oxidation.
[d] Washed with $CHCl_3$.
[e] Washed with H_2O.

According to empirical evidence for cation location, based on the relative peak heights in a powder diffraction pattern for a zeolite (*29*), cations are randomly distributed within the large cavities if $I_{(331)} \gg I_{(220)} > I_{(311)}$, whereas cations are located at sites II and I′ if $I_{(331)} > I_{(311)} \geq I_{(220)}$. Cations are located primarily at site I if $I_{(311)} > I_{(220)} > I_{(331)}$. Using these empirical criteria, the diffraction patterns of the molybdenum-exchanged zeolites suggest that the molybdenum ions are probably located at S_{II} sites in the large cavities.

XPS study. Table 2 summarizes the Si_{2p}, Al_{2s}, Al_{2p}, and O_{1s} binding energies for these elements in several samples. All of the binding energies remained constant in the fresh and used samples within experimental error (±0.3 eV). The XPS results are in good agreement with the values reported by other investigators for zeolites (*30, 31*).

A representative Mo_{3d} spectrum of a fresh molybdenum-exchanged zeolite, $Mo_{1.6}HY_u$, is shown in Fig. 5a. All of the fresh samples had the same peak shape and binding energies. The latter for the $Mo_{3d_{3/2}}$

TABLE 2

Binding Energies from XPS of Molybdenum-Containing Zeolites[a]

Catalyst	Si_{2p}	Al_{2s}	Al_{2p}	C_{1s}	O_{1s}	$Mo_{3d_{5/2}}$	$Mo_{3d_{3/2}}$
$MoCl_5/NaY$	102.7	119.4	74.6	284.4	532.2	232.9	236.0
$Mo_{1.6}HY_u$	102.7	119.8	74.7	284.6	532.3	232.7	235.8
$Mo_{1.2}HY$	102.9	119.6	74.7	284.3	532.7	232.7	235.8
$Mo_{1.6}Co_{3.5}HY$	102.7	119.7	74.9	284.9	532.2	232.6	235.8
HY_u	102.8	119.7	75.0	—	532.4	—	—

[a] For catalyst samples, the Si_{2s} line from the zeolite was used as a secondary binding energy reference and was assigned a value of 154.0 eV relative to the gold $Au_{4f_{7/2}}$ peak, which was taken as 84.0 eV.

and $Mo_{3d_{5/2}}$ were 235.8 ± 0.2 and 232.7 ± 0.2 eV, respectively, which indicates that the molybdenum ions in the fresh zeolite catalysts were mainly present as Mo(VI) (*19, 32*). The full width at half-maximum (FWHM) of the $Mo_{3d_{5/2}}$ peaks was about 2.5 eV, which is greater than that of Mo_2Cl_{10} having a value of 1.5 eV (*33*). This broadening effect could be due to the interaction of the support with Mo ions.

The Mo_{3d} spectrum for fresh $Mo_{3.7}Co_{3.5}HY$, shown in Fig. 5b, is characterized by three resolved peaks. The additional peak at a lower binding energy of 228.2 eV is near to that of the $Mo_{3d_{5/2}}$ line of Mo(II) (*33*). This peak appeared for samples having an Mo loading greater than 2.9Mo/u.c. The $Mo_{3d_{3/2}}$ peak for Mo(II) would be expected to appear as a shoulder on the peak at 232.7 eV, which is evident in Fig. 5b. These results indicate that all of the Mo oxidation states ranging from Mo(II) to Mo(VI) could be present in the fresh $Mo_{2.9}Co_{3.9}HY$ and $Mo_{3.7}Co_{3.5}HY$ zeolites. After the cyclohexene oxidation, all of the low-valent molybdenum ions in the spent catalyst of $Mo_{3.7}Co_{3.5}HY$ zeolite were oxidized to Mo(VI) as shown in Fig. 5c.

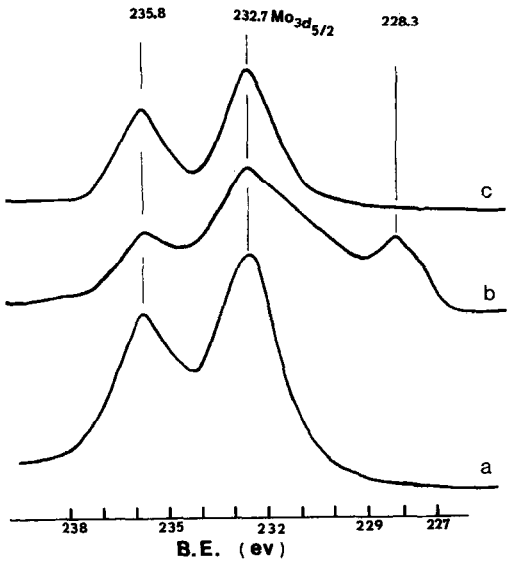

FIG. 5. Mo_{3d} XPS spectra of (a) fresh $Mo_{1.6}HY_u$ zeolite; (b) fresh $Mo_{3.7}Co_{3.5}HY$ zeolite; and (c) used $Mo_{3.7}Co_{3.5}HY$ catalyst.

The Cl_{2p} spectrum was not observed in any molybdenum-exchanged zeolite. In the sample that contained molybdenum chloride support on NaY zeolite, the Cl_{2p} line, characterized by a $Cl_{2p_{1/2,3/2}}$ doublet with binding energies of 199.4 and 198.0 eV, was observed (*33*). In Figs. 6a and b spectra of Co_{2p} peaks are compared for a fresh $Mo_{1.6}Co_{6.6}HY$ and a used $Mo_{1.6}Co_{3.5}HY$ zeolite catalyst. The Co_{2p} lines consist of two primary peaks at 781.6 and 797.8 eV for the $2p_{3/2}$ and $2p_{1/2}$ levels. Satellite lines were also observed at binding energies 5.0 eV greater than the primary lines. The spin–orbit splitting of 16 eV for the Co_{2p} lines, accompanied by pronounced satellite structure, is characteristic of paramagnetic Co(II) (*34, 35*). Therefore, the XPS spectra provide strong evidence that most of the

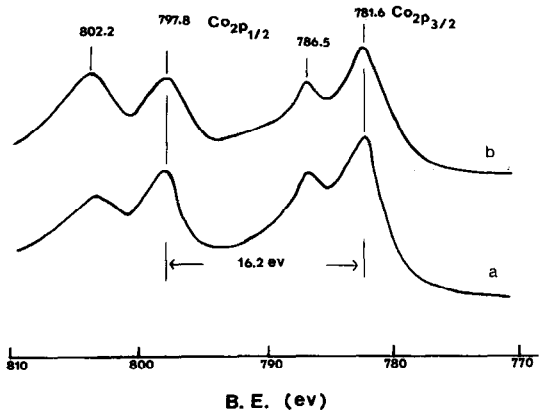

FIG. 6. Co_{2p} XPS spectra of (a) fresh $Mo_{1.6}Co_{6.6}HY$ zeolite and (b) used $Mo_{1.6}Co_{3.5}HY$ catalyst.

cobalt was present as Co(II) ions after the cyclohexene oxidation had occurred.

The relative surface concentration of Mo, indicated by the $Mo_{3d_{5/2}}/Si_{2s}$ ratio, for various molybdenum-containing zeolites, both before and after the cyclohexene oxidation, is listed in Table 3. It can be seen that the Mo/Si ratio for the impregnated sample, denoted by 2.64 wt% $MoCl_5$/NaY, is about sevenfold greater than that for the exchanged sample, $Mo_{1.6}Co_{3.6}HY$, which had the same weight percentage of Mo. One may conclude that the solid–solid exchange reaction indeed resulted in exchange of Mo into the zeolites.

Upon comparing the Mo/Si ratio for the fresh $Mo_{1.6}Co_{3.5}HY$ catlayst with a used one, it was found that Mo ions tend to migrate toward the external surface of the zeolite during the cyclohexene oxidation, particularly at a reaction temperature of 75°C. For catalysts having higher Mo loadings ($Mo_{2.9}Co_{3.9}HY$ and $Mo_{3.7}Co_{3.5}HY$) there was almost no change in the Mo/Si ratio after the cyclohexene oxidation. Moreover, the Mo/Al ratio for the impregnated sample is approximately the same as those ratios for the used $Mo_{1.6}Co_{3.5}HY$ zeolite at 75°C and the fresh $Mo_{3.7}Co_{3.5}HY$ zeolite. These results suggest that at higher loadings all of the exchange sites on the external surface were occupied by the molybdenum ions, thus no additional migration to the surface occurred. The $Mo_{3d_{5/2}}/Si_{2s}$ surface ratio determined by XPS for the fresh $Mo_{1.6}Co_{3.5}HY$ zeolite was about half of the theoretical value that was calculated by assuming a uniform distribution of Mo in the zeolite. For the higher loadings ($Mo_{2.9}Co_{3.9}HY$ and $Mo_{3.7}Co_{3.5}HY$), the surface ratios were approximately equal to the theoretical values as indicated in Table 3. It appears, therefore, that the molybdenum ions in the fresh $Mo_{1.6}Co_{3.5}HY$ catalyst are probably concentrated at sites more than 20Å within the zeolite crystallites.

Table 4 summarizes the surface ratios Al_{2s}/Si_{2p} for various molybdenum-exchanged zeolites, HY_u, and NaY zeolites. In comparison with the Al/Si ratio for the NaY zeolite, a slight increase in surface aluminum concentration was noted for all of the Mo-exchanged HY and MoCoHY zeolites. Defosse *et al.* (*36*) have demonstrated that when ion exchange caused a

TABLE 3

Surface Mo Concentration Ratio of Molybdenum-Containing Zeolites before and after Cyclohexene Oxidation

Sample	Reaction temperature (°C)	$Mo_{3d_{5/2}}/Si_{2s}$	
		Before	After
2.64 Wt% $MoCl_5$/NaY	—	0.037	—
$Mo_{1.6}Co_{3.5}HY$	55	0.007	0.015
$Mo_{1.6}Co_{3.5}HY$	75	0.007	0.030
$Mo_{2.9}Co_{3.9}HY$	65	0.018	0.020
$Mo_{3.7}Co_{3.5}HY$	65	0.028	0.028

TABLE 4

Surface Al/Si Ratio for Various Zeolites

Sample	Al_{2s}/Si_{2p}	Sample	Al_{2s}/Si_{2p}
NaY	0.24	$Mo_{1.6}Co_{3.5}HY$	0.27
HY_u	0.46	$Mo_{2.9}Co_{3.9}HY$	0.29
$Mo_{1.6}HY_u$	0.63		
$Mo_{1.2}HY$	0.30	$Mo_{3.7}Co_{3.5}HY$	0.28

partial loss of crystallinity, the superficial concentration of aluminum increased in Y zeolites. Hence, the relatively higher Al_{2s}/Si_{2p} ratio for MoHY and MoCoHY zeolites could be attributed to degradation of the framework of zeolite. For ultrastable Y zeolites the surface Al/Si ratio was twice that observed for NaY zeolite. Our results, which are in good agreement with those of several recent studies (*30, 36*), demonstrate that superficial enrichment in aluminum occurs in the preparation of ultrastable Y zeolites. Structural studies have shown that ultrastable Y zeolites can contain a variety of exchangeable aluminum species such as $Al(OH)_2^+$, $Al(OH)^{2+}$, and AlO^+ (*37–39*). It is reasonable to assume that some of these aluminum ions come out of the lattice and act as cations at the surface, thus leading to the enrichment in surface aluminum concentration. The solid–solid exchange reaction of HY_u zeolite with $MoOCl_4$ resulted in a further increase in the surface Al_{2s}/Si_{2p} ratio.

A model for Mo ions in Mo-exchanged zeolites. Since the molybdenum-exchanged Y zeolites are active in the decomposition of *tert*-butylhydroperoxide and epoxidation of cyclohexene with molecular oxygen, one may conclude that the heterogeneous molybdenum species are accessible to those reactant molecules and the coordination of the Mo ion is not complete. The XPS and EPR results indicate that Mo ions are located on the external surface and within the zeolite cavities. As suggested by the X-ray diffraction results the molybdenum ions may occupy S_{II} sites in the large cavities where trigonal symmetry exists. Tetrahedral coordination would result, in which the molybdenum ion would lie on the axis of the hexagonal ring connecting the large cavity with the sodalite cage. As mentioned above, at least part of the molybdenum ions in MoHY and MoCoHY zeolites have a Mo=O bond, but no such bond is evident in $MoHY_u$ zeolites. It is, therefore, reasonable to postulate the structures of molybdenum ion in the Mo-exchanged Y zeolites:

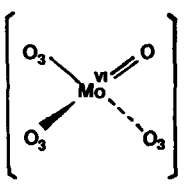

(I)

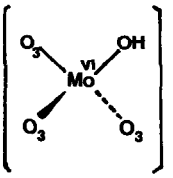

(II)

In these models molybdenum ions are believed to be located at S_{II} sites. Furthermore both the oxo and hydroxy groups extend into the large cavities, which would allow more effective coordination between Mo and other ligands that are introduced during the catalytic oxidation of cyclohexene. Model (I) is assigned to Mo ions in MoHY and MoCoHY, whereas model (II) presumably occurs in $MoHY_u$ zeolites. The presence of oxo and hydroxy groups is not only consistent with the exchange stoichiomtry and spectroscopic data, but it is also consistent with the coordination chemistry of molybdenum. In this respect it is unlikely that Mo(VI) would be coordinated only to three oxygen ligands, with each having an effective total charge of -1.

CONCLUSIONS

The solid–solid exchange reaction of hydrogen Y zeolites with molybdenum oxytetrachloride is an effective means of introducing Mo ions into a zeolite; however, some loss in crystallinity occurs. Prior to the catalytic epoxidation, molybdenum ions were observed in several oxidation states, but after the reaction only Mo(VI) was detected. Molybdenum in the form of $(Mo(VI)=O)^{4+}$ and $(Mo(VI)—OH)^{5+}$ complex ions is postulated to be located as S_{II} sites.

ACKNOWLEDGMENTS

This work was supported by the National Science Foundation under Grant CHE-7706792. The adsorption data were obtained by Mr. Donald Beck.

REFERENCES

1. Landau, R., *Hydrocarbon Process.* **46**, 141 (1967).
2. Stobaugh, R. B., Calarco, V. A., Morris, R. A.,

and Stroud, L. W., *Hydrocarbon Process.* **52,** 99 (1973).
3. Eberly, P. E., and Kimberlin, C. N., *Advan. Chem. Ser.* **102,** 374 (1971).
4. Rouchaud, J., and Fripiat, J., *Bull. Soc. Chim. Fr.* **1,** 78 (1969).
5. Wilhelm, F. C., "Preparation and Characterization of Mo-Containing Zeolites," Climax Report L-287-51, March 15, 1977.
6. Bukata, S. W., Castor, C. R., and Milton, R. M., U.S. Patent 3,013,988 (Union Carbide), (1966).
7. Gallezot, P., Coudurier, G., Primet, M., and Imelik, B., *Amer. Chem. Soc. Ser.* **40,** 144 (1977).
8. Clearfield, A., Saldarriaga, C. H., and Buckley, R. C., *in* "Third International Conference on Molecular Sieve, Zurich, Switzerland," (J. B. Uytterhoeven, Ed.), p. 241 (1973).
9. Clearfield, A., and Troup, J. M., *J. Phys. Chem.* **74,** 2578 (1970).
10. Scherzer, J., and Bass, J. L., *J. Catal.* **46,** 100 (1977).
11. Scherzer, J. and Rutter, R. E., *Ind. Eng. Chem. Prod. Res. Develop.* **17,** 219 (1978).
12. Dai, P. E., and Lunsford, J. H. *J. Catal.* **64,** 184 (1980).
13. McDaniel, C. V., and Maher, P. K., *in* "Conf. Mol. Sieves, 1967," *Soc. Chem. Ind. London* Monogr. 186 (1968).
14. Carten, W. J., Schweitzer, G. K., and Carlson, T. A., *J. Electron Spectrosc. Relat. Phenom.* **5,** 825 (1974).
15. Scofield, J. H., *J. Electron Spectrosc. Relat. Phenom.* **8,** 129 (1976).
16. Mallock, A. K., *Inorg. Synth.* **10,** 54 (1967).
17. Uytterhoeven, J., Christner, L. G., and Hall, W. K., *J. Phys. Chem.* **69,** 2117 (1965).
18. Che, M., MacAteer, J. C., and Tench, A. J., *Chem. Phys. Lett.* **31,** 145 (1975).
19. Ward, M. B., Lin, M. J., and Lunsford, J. H., *J. Catal.* **50,** 306 (1977).
20. Abdo, S., Lojacono, M., Clarkson, R. B., and Hall, W. K., *J. Catal.* **36,** 330 (1975).
21. Howe, R. F., and Leith, I. R., *J. Chem. Soc. Faraday Trans. I* **69,** 1967 (1973).
22. Scherzer, J., and Bass, J. L., *J. Catal.* **28,** 101 (1973).
23. Flanigen, E. M., *in* "Zeolite Chemistry and Catalysis" (J. A. Rabo, Ed.), *ACS Monogr.,* Vol. 171, p. 80 (1976).
24. Pichat, P., Beaumont, R., and Barthomeuf, D., *J. Chem. Soc. Faraday Trans. I* **70,** 1402 (1974).
25. Primet, M., *J. Chem. Soc. Faraday Trans. I* **74,** 2570 (1978).
26. Mitchell, P. C. H., and Trifiro, F., *J. Chem. Soc. A,* 3183 (1970).
27. Cotton, F. A., and Wing, A. M., *Inorg. Chem.* **6,** 867 (1965).
28. Flanigen, E. M., Khatami, H., and Szymanski, H. A., *Advan. Chem. Ser.* **101,** 201 (1971).
29. Pearce, J. R., private communication.
30. Vedrine, J. C., Dufaux, M., Naccache, C., and Imelik, B., *J. Chem. Soc. Faraday Trans. I.* **74,** 440 (1978).
31. Pedersen, L. A., and Lunsford, J. H., *J. Catal.* **61,** 39 (1980).
32. La Ginestra, A., Ferragina, C., Correnti, S., Cicconetti, L. Mattogono, G., and Battistoni, C., *Gazz. Chim. Ital.* **103,** 963 (1973).
33. Walton, R. A., *in* "Proceedings of the Climax Second International Conference on the Chemistry and Uses of Molybdenum" (P. C. H. Mitchell, Ed.), Climax Molybdenum Company, Ltd., London, p. 34 (1977). *Note added in proof:* A similar binding energy observed for MoO_2 has been attributed to pairs of Mo(IV) ions which have a double bond between the metal atoms. Haber, J., Marczewski, W., Stoch, J., and Ungier, L., Ber. Bunsenges. *Physik. Chem.* **79,** 970 (1975); Broclawik, E., Foti, A., E., and Smith, V. H., *J. Catal.* **62,** 187 (1980).
34. Briggs, D., and Gibson, V. A., *Chem. Phys. Lett.* **25,** 493 (1974).
35. Lunsford, J. H., Hutta, P. J., Lin, M. J., and Windhorst, K. A., *Inorg. Chem.* **17,** 606 (1978).
36. Defosse, C., Delmon, B., and Canesson, P., *Amer. Chem. Soc. Symp. Ser.* **40,** 86 (1977).
37. Maher, P. K., Hunter, F. D., and Scherzer, J., *Advan. Chem. Ser.* **101,** 266 (1971).
38. Kerr, G. T., *J. Phys. Chem.* **71,** 4155 (1967).
39. Jacobs, P. A., and Uytterhoeven, J. B., *J. Chem. Soc. Faraday Trans. I* **69,** 2117 (1973).